Taxonomy of *Nephroselmis viridis* sp. nov. (Nephroselmidophyceae, Chlorophyta), a sister marine species to freshwater *N. olivacea*

Haruyo Yamaguchi[1], Shoichiro Suda[2], Takeshi Nakayama[1], Richard N. Pienaar[3], Mitsuo Chihara[1] and Isao Inouye[1].

[1]Graduate School of Life and Environmental Sciences, University of Tsukuba, Tsukuba, Ibaraki 305-8572, Japan,

[2]Department of Chemistry, Biology and Marine Science, University of the Ryukyus, Nishihara, Okinawa 903–0213, Japan.

[3]School of Animal, Plant and Environmental Sciences, University of the Witwatersrand, Private Bag 3, Johannesburg, WITS 2050, South Africa.

Correspondence to: Isao Inouye.

E-mail: iinouye@sakura.cc.tsukuba.ac.jp

Abstract

The genus *Nephroselmis* (Nephroselmidophyceae), which had been placed in the Prasinophyceae, is one of the primitive green flagellates that are important to our understanding of the early evolution of green plants. We studied a new species of *Nephroselmis* isolated from Japan, Fiji and South Africa. This species has been known for a long time as undescribed species '*N. viridis*.' *N. viridis* possesses some ultrastructural characters shared with only the freshwater type species *N. olivacea*, including a disc-like structure beneath the pyrenoid and bipolar spiny body scales with 1-5-8-5-1 spines. Molecular phylogenetic analysis based on 18S rDNA also supports a sister relationship between *N. viridis* and *N. olivacea*. However, *N. viridis* is distinguishable from *N. olivacea* by the shape of its starch sheath, its scales, its pigment composition and its habitat. In this paper, we designate the formal description of *N. viridis* sp. nov. We also describe variability in the 18S rDNA introns of various *N. viridis* strains. This detailed study of *N. viridis* provides some insights into the evolution of *Nephroselmis*.

Keywords

18S rDNA · intron · *Nephroselmis viridis* · phylogeny · Prasinophyceae · ultrastructure

Introduction

The green algae traditionally classified in the Prasinophyceae are important components of coastal phytoplankton communities, but a few species are also common in freshwater. Most prasinophycean algae are unicellular flagellates possessing a scaly covering, depressions from which flagella emerge and an asymmetrical cell architecture (Sym and Pienaar 1993). However, these characters have been considered to be symplesiomorphies of the green plants (Viridiplantae) (e.g., Moestrup and Ettl 1979; Melkonian 1984, 1990; Sym and Pienaar 1993). Recent molecular phylogenetic studies support the paraphyletic nature of the Prasinophyceae (e.g., Steinkötter et al. 1994; Nakayama et al. 1998; Fawley et al. 2000; Guillou et al. 2004; Turmel et al. 2009). The Prasinophyceae have been reinvestigated and a number of new classes, including the Nephroselmidophyceae ('Nephrophyceae'), have been proposed (Cavalier-Smith 1993; Marin and Melkonian 1999, 2009; Massjuk 2006). Information on the diversity of the prasinophycean algae is indispensable for understanding the early evolution of the Viridiplantae. However, phylogenetic relationships among prasinophycean algae have

been only partially resolved. Furthermore, many undescribed prasinophycean algae still exist in nature (e.g., Fawley et al. 2000; Guillou et al. 2004; Viprey et al. 2008).

The *Nephroselmis*, one of the genera previously classified into the Prasinophyceae, is presently the sole member of the class Nephroselmidophyceae (Nakayama et al. 2007). The cell of *Nephroselmis* is laterally compressed (along the right–left axis) and has two flagella inserted laterally (ventrally) (e.g., Moestrup and Ettl 1979). The cell body and flagella are covered by various scales (e.g., Sym and Pienaar 1993; Marin and Melkonian 1994; Nakayama et al. 2007). The cell possesses a single cup-shaped chloroplast with a pyrenoid and an eyespot. The majority of the described and undescribed species of *Nephroselmis* are marine (Suda 2003; HY and SS unpublished). However, the type species of the genus, *N. olivacea* Stein, occurs in freshwater. *N. olivacea* is common in ponds, lakes and paddy fields all over the world (e.g., Moestrup and Ettl 1979). However, the relationship between marine species and *N. olivacea* is not well understood.

We studied in detail some strains of a new species of *Nephroselmis* isolated from coastal waters of Japan, Fiji and South Africa. This species has been known as an undescribed species for a long time. Many ultrastructural characters suggest that the

species is closely related to *N. olivacea*. Molecular phylogenetic analysis also indicated a sister relationship between these species. Based on these results, we propose the name *N. viridis* sp. nov. for this species and provide a formal description.

Materials and methods

Sampling and culturing

In this study, five strains of *Nephroselmis viridis* were used. Strains NIES-486 and PS535 were isolated from sediment collected at Harima-Nada, Hyogo Prefecture, Japan in 1983 and 1985, respectively. MBIC 10871 was collected from a surface water sample at the Republic of the Fiji Islands in 1993. Inshore waters collected from off the Natal coast, Kwa-Zulu Natal, South Africa in 1984 were used for SA. Saeki-L was isolated from surface waters at Saeki port, Oita Prefecture, Japan in 1997. Clonal cultures were established by micropipetting from Erd-Schreiber modified (ESM) medium (Kasai et al. 2009)-enriched samples and were maintained in the same medium (*c*. 30‰ salinity) at 20°C under 25 to 50 μmol photon m^{-2} s^{-1} with a 14 h : 10 h or a 12 h : 12 h (light : dark)

cycle. NIES-486 is now deposited in the Microbial Culture Collection of the National Institute for Environmental Studies, Tsukuba, Japan. Unfortunately, the other strains have been lost.

Morphological observations

For light microscopy, a Nikon Optiphot (Nikon, Tokyo, Japan) and a Leica DMRD (Leica Microsystems, Wetzlar, Germany) both equipped with differential interference contrast (DIC) optics were used. Whole mount preparations were made using the method of Moestrup and Ettl (1979) or Marin and Melkonian (1994). Materials for thin sections were prepared as follows. Equal volumes of fixative [5% glutaraldehyde, 0.5 M sucrose, in 0.2 M cacodylate buffer (pH 7.2)] and culture medium containing actively growing cells were mixed together at room temperature for 1–2 h. After rinsing twice with 0.1 M cacodylate buffer, cells were postfixed in 2% osmium tetroxide in 0.1 M cacodylate buffer for 1–2 h. Cells were embedded in Spurr's resin (Spurr 1969) after dehydration in a graded ethanol series. Sections were cut with a diamond knife, collected onto formvar-coated slot grids and double stained with 2% uranyl acetate and

lead citrate (Reynolds 1963). Observations were carried out with a JEM 100C and JEM 100CXII transmission electron microscope (JEOL, Tokyo, Japan). Materials for scanning electron microscopy (SEM) were fixed with 2.5% glutaraldehyde containing 0.25 M sucrose. Cells were placed on an SEM plate coated with poly-L-lysine, rinsed, dehydrated in a graded ethanol series and then substituted with isoamyl acetate prior to critical-point drying with a HP-20 (Hitachi, Tokyo, Japan). Specimens were examined with an HHS-2R scanning electron microscope (Hitachi, Tokyo, Japan) after sputter coating with gold. The directions of the cell and numbering system of the flagella and microtubular roots follow Moestrup (2000) and Nakayama et al. (2007). The terminology for the hair scales follows Marin and Melkonian (1994).

PCR, sequencing, phylogenetic analysis and intron identification

Total DNA was extracted from strains NIES-486, PS535 and MBIC10871 using a GenomicPrep Cells and Tissue DNA isolation Kit (GE Healthcare Japan, Tokyo) according to the manufacturer's instruction. 18S rDNA sequences were amplified using polymerase chain reaction (PCR) with previously reported primers (SR1–12 in

Nakayama et al. 1998). PCR products were directly sequenced using an ABI 377 autosequencer (Applied Biosystems, Inc., Foster City, USA) with a BigDye Terminator v3.1 Cycle Sequencing Kit (Applied Biosystems) and the same primers. Sequences of 18S rDNA were deposited in the DNA Data Bank of Japan (DDBJ). Sequences were manually aligned after a preliminary alignment using MAFFT v 6.240 through GenomeNet (http://align.genome.jp/mafft/) with default settings. Because the sequences of NIES-486 and PS535 included some group I introns, only sequences of the exon were used for the phylogenetic analysis. The positions of the introns were defined as proposed by Johansen and Haugen (2001). For the phylogenetic analysis, nucleotide sequences excluding ambiguously aligned regions were used (1,758 sites). Trees were constructed by the maximum likelihood (ML) method as reported previously in Yamaguchi et al. (2010). The sequences of *Pyramimonas olivacea* Carter and *Pseudoscourfieldia marina* (Throndsen) Manton were used as the outgroup because a preliminary analysis using a larger data set including more chlorophytes indicated monophyly of *Nephroselmis* with *N. viridis* (not shown).

Description

Nephroselmis viridis Inouye, Pienaar, Suda et Chihara sp. nov.

Cellula complanata, phaseoliformis, 5.5–9 µm longa, 5–8 µm lata, 3–5 µm crassa. Flagella duo, inaequalia, heterodynamica, in ventrali inserta. Flagellum longum volubile in cellula quiescenti. Chloroplastus unus, viridis, parietalis, dorsalis, cum stigmate ventrali. Pyrenoides cum structura discoidea, vagina amylacea cupuliformi, thylacoidetibus complanatis. Squamae corperis tegentes pentamorphae; squamae stati primi parvae, quadratae; squamae stati secundi parvae, hanakaku-formes; squamae stati terti spiniferae, circa 120 nm in diametro, unipolares, cun 11 spinis. Flagella sine squama stati terti. Squamae T-piliformes sine submonibus proximalibus. Pilus foveae et pilus apices absentes.

Cells flattened, bean-shaped, 5.5–9 μm long, 5–8 μm wide and 3–5 μm thick. Two unequal heterodynamic flagella, inserted ventrally. The long flagellum coiling in the resting cell. A single chloroplast, greenish, parietal, dorsal, with a conspicuous pyrenoid and a ventral eyespot. Pyrenoid with a disc-like structure, cup-shaped starch sheath and thylakoid sheets. Body scales are four types; innermost layer scales small, square; second layer scales small, Hanakaku-shaped; large spiny scales *c*. 180 nm in diameter,

unipolar, with 11 spines. Flagella with a third layer of stellate scales. T-hairs with proximal subunits. Pit and tip hairs absent.

Holotype: TNS-AL-56966 for the strain NIES-548 at the Department of Botany, the National Museum of Nature and Science, Japan. The strain NIES-486 used for the holotype is maintained at the National Institute of Environmental Studies, Tsukuba, Japan.

Type locality: Sediment from the Sea of Harima, Hyogo Prefecture, Japan.

Paratype: TNS-AL-56967 for the strain PS535, and TNS-AL-56968 for the strain MBIC 10871 at same place to the holotype. RYUA0003 for a duplicate block of the strain MBIC 10871 at the herbarium of the Faculty of Science, University of the Ryukyus, Okinawa (RYUA).

Etymology: The specific epithet refers to the color of the chloroplast, which is different from the closely related species *N. olivacea*.

Results

Cell structure

The cell structure of all strains was almost identical at both the light and the electron microscopic levels. Although they exhibited some differences in cell size, the values overlapped with one another. The cells of *N. viridis* are flattened in the right–left axis and bean-shaped in lateral view (Figs. 1, 2a–d). The dorsal side of the cell is rounded, while in ventral view, the cell is flattened and has a central shallow groove surrounded by four low projections (Fig. 2c, d). The cell shape is roughly symmetrical in the anterior–posterior and right–left axes. Two flagella emerge from the ventral groove (Fig. 2a, d). The long (no. 1) flagellum is *c*. 3–4 times the cell length and the short (no. 2) flagellum is approximately 1–1.5 times the cell length. In the swimming cell, the long flagellum beats posteriorly, while the short flagellum beats anteriorly (Fig. 1d; Inouye and Hori 1991 as *N*. aff. *rotunda*). When the cell comes to rest, both flagella coil along the cell body (Fig. 1a, b, e). When at rest, the cell usually attaches its left side to the substratum, as does *N. anterostigmatica* Nakayama et al. (Nakayama et al. 2007). The cells reproduce by bisection. The occurrence of cells in sediment samples suggests the presence of cysts as in *N. olivacea* (Suda et al. 1989, 2004), but sexual reproduction and cyst formation were not observed.

Actively growing cells of *N. viridis* are grass green, but yellowish green in older cultures. The cell possesses a parietal cup-shaped chloroplast lying against the dorsal side of the cell (Figs. 1, 2a, c). On both the right and the left sides of the chloroplast, there is a wide sinus (Figs. 1b, 2b, 3a). The thylakoids usually form lamellae composed of two or three thylakoids, but lamellae with four or more thylakoids are frequently observed (Figs. 2a–c, e, f, 3a). On the central region of the chloroplast cavity there is a small chloroplast bulge, in which tubular structures of about 14–20 nm in diameter are sometimes observed (Fig. 2a, c, e). These tubules often attach to the inner chloroplast membrane. A similar structure has been reported in various algae (e.g., Hoffmann 1967; Pickett-Heaps and Fowke 1970), but its function is unclear. At the base of the bulge, in addition to the anterior and posterior part of the chloroplast and in the same plane, a translucent region is frequently observed (Fig. 2a, c, e). The pyrenoid has a cup-shaped starch sheath and is situated at the dorsal portion of the chloroplast (Figs. 1, 2a, c). Several thylakoid lamellae arranged in parallel intrude into the pyrenoid matrix from the edge of the starch sheath (Fig. 2a, c). The thylakoid lamellae in the pyrenoid matrix are usually reduced to single thylakoids (Fig. 2a, c, f). Thylakoids from the opposite side of the opening occasionally continue into the pyrenoid matrix, thus they exhibit a

U-shaped track (Fig. 2f). A characteristic disc-like structure is situated in the narrow space between the starch sheath and the dorsal margin of the chloroplast (Fig. 2a, c, f). This structure is divided into two parts: a ventral part containing an array of indistinct tubular structures arranged perpendicularly to the anterior–posterior / right–left axes, and a translucent dorsal part devoid of tubules (Fig. 2f). An eyespot composed of many globules arranged in a single layer is situated at the anterior-ventral side of the chloroplast (Figs. 1, 2a, 3a, S1f). There is a nucleus in the right side of the cell (Figs. 2b, c, 3a, S1). Ramified cisternae of rough endoplasmic reticulum (ER) extend from the nuclear envelope and are distributed on the left side of the cytoplasm as well as just beneath the plasma membrane (Figs. 2b, c, 3a, S1f). Fibrous material is sometimes observed within these cisternae (Fig. S1e; Sym and Pienaar 1993). Mitochondrial profiles with flat cristae are usually located along the inner surface of the chloroplast cavity (Figs. 2a, b, c, 3a, S1). Observations of serial sections suggest that they represent a single reticulate mitochondrion. The microbody is elongated ventrally from the bulge of the chloroplast along the rhizoplast (Fig. 2a, c, e). The Golgi body is situated on the left side of the cytoplasm (Figs. 2c, 3a). The maturing face of the Golgi body is oriented to the ventral groove of the cell and an extension of the nuclear envelope is situated

along the forming face. The Golgi vesicles sometimes include various scale types (Fig. 3a). A large vacuole usually containing scales is always situated in the ventral left portion of the cell (Figs. 2b, S1a–d). This position is comparable to that of the contractile vacuole in *N. olivacea* (Moestrup and Ettl 1979), but the vacuole is not contractile in *N. viridis*. Rows of globular or discoid subunits (*c*. 20 nm in diameter) are frequently observed at both the anterior and posterior sides in the chloroplast cavity (Fig. 2b). These rows are 400–800 nm in length and arranged regularly in a three-dimensional bundle. The rows are arranged parallel to each other in longitudinal sections (Fig. 3b). In transverse sections every four rows are arranged in the shape of a cross (Fig. 3c). Because the size of the subunit is comparable to that of a ribosome (but it is flatter), this structure may be a bundle of polysomes.

The ultrastructural details of the flagellar apparatus can be found in Supplementary Material online.

Scaly covering

All strains possess a similar scaly covering. However, some variation was detected,

especially in the large spiny scales and the hair scales (see below). In all strains, three layers of scales cover the entire cell body (Fig. 4a–c, e). The innermost layer just above the plasma membrane is composed of small square scales with a distinct central boss (*c*. 45 nm in diameter) (Figs. 4a–c, e, 5a). In the second layer, the small scales are located regularly on top of the interval between the innermost scales. The scales of the second layer are square (*c*. 45 nm in diameter) and have a central boss and four thick rhomboidal or arrow-like corners (Figs. 4a–c, e, 5b). We call this type of scale a Hanakaku (one of the Japanese heraldic family symbols) scale. The scales forming the third layer are unipolar spiny scales composed of a central spine and two tiers of rays, each of which consists of five spines (Figs. 4a–f, 5c). Thus, this type of spiny scale has a total of 11 spines. The size and thickness of the spines of the spiny scales vary among and within strains (Fig. 4e, f, Table 1), and occasionally even within a cell (not shown). In some strains, the third layer is overlaid by a bipolar type of spiny scale (Fig. 4a, c). This type of scale consists of a central ray with eight spines sandwiched between two rays composed of five spines, as well as a proximal and a distal spine, making a total of 20 spines (Figs. 4d, 5d). The bipolar spiny scales are restricted around the ventral groove or are completely absent in some strains (Table 1). The bipolar spiny scales were

commonly observed in NIES-486 just after the establishment of the culture, but the strain lost this scale in 1990.

The flagella of *N. viridis* are covered by three scaly layers (Figs. 4g, h). The innermost layer is composed of pentagonal scales (Figs. 4g, h, 5e). The second layer is made up of rod-shaped scales with some tiny projections (Figs. 4d, g, h, 5f). The rod-shaped scales are overlaid by small stellate scales with 11 spines (*c*. 100 nm in diameter) (Figs. 4g, h, 5g). The basic architecture of this type of scale is identical to that of the third layer body scales, and the anterior spine is not curved as in *N. olivacea* (Moestrup and Ettl 1979). Two types of hair scales, T-hairs and P_1-hairs, are attached to the flagella. T-hairs are distributed along the entire length of both flagella (Figs. 4g, 6a). Each T-hair is 500–550 nm long and consists of a proximal filament, a shaft, a row of proximal and distal subunits, and a short distal filament (Figs. 6b–f, 7a). The numbers of proximal and distal subunits vary among strains (Fig. 6b–f, Table 1). P_1-hairs ornament only the short no. 2 flagellum (Fig. 6a). Each P_1-hair is *c*. 2.2 μm long and consists of a proximal wedge, a shaft with a rough appearance and a row of central and distal subunits (Figs. 6g, h, 7b). The numbers of central and distal subunits also vary among strains (Table 1).

18S rDNA introns and phylogenetic analysis

18S rDNA sequences were obtained from three strains: MBIC 10871, NIES-486 and PS535. Whereas no intervening sequence was observed in the 18S rDNA of MBIC 10871, two and three intervening sequences were observed in the 18S rDNA of NIES-486 and PS535, respectively (Fig. 8a). The insertion positions of these two intervening sequences (S324 and S989) were identical between NIES-486 and PS535. In addition, the intervening sequences were nearly identical in the two strains (only one nucleotide was different). Based on the comparison of core sequences, these were probably group I introns, which are known to exist in the rDNA of many eukaryotes (Burke et al. 1987; Haugen et al. 2005). The sequences excluding putative introns were almost identical among the strains, and only a single indel was detected in MBIC 10871.

A phylogenetic analysis based on 18S rDNA was performed including the new sequences from MBIC 10871, NIES-486 and PS535. Intron sequences were removed for the subsequent phylogenetic analysis. Because a preliminary analysis demonstrated

that these strains appeared to be included within *Nephroselmis*, only phylogenetic relationships within the genus were analyzed in this study (Fig. 8b). The sequences from the three strains of *N. viridis* formed a robust clade (100% bootstrap probability [BP]) and it was a sister to *N. olivacea* (100% BP). A clade (100% BP) containing *N. spinosa* Suda and *Nephroselmis* sp. (MBIC 11149) was a sister to a clade containing *N. viridis* and *N. olivacea,* but the BP was low (38%). A clade (100% BP) containing *N. anterostigmatica* and *N. astigmatica* Inouye et Pienaar was situated next in the tree. At the base of the genus, *N. pyriformis* (N. Carter) Ettl diverged with moderate support (65% BP).

Discussion

Taxonomy of *Nephroselmis viridis*

The alga reported in this study has been known as '*Nephroselmis viridis*' since Sym and Pienaar (1993) cited the locally used name for it in their review article. This alga was also referred to in previous studies as *N.* aff. *rotunda* (Inouye and Hori 1991) and

Nephroselmis sp. (Young and Pienaar 1989; Yoshii et al. 2005). It has, however, never been formally described. Thus, this paper provides the formal description of this species.

N. viridis is undoubtedly a member of the genus *Nephroselmis* because of its laterally compressed cell, its two ventrally inserted heterodynamic unequal flagella, its eyespot situated at the anterior ventral side of the chloroplast and its characteristic scaly covering. Molecular phylogenetic analysis also supports this classification. Among marine species, *N. rotunda* (Carter) Fott, *N. spinosa*, *N. minuta* (Carter) Butcher and *N. gaoae* Tseng et al. resemble this alga in their cell shape and in their coiling flagella (Carter 1937; Butcher 1959; Manton et al. 1965; Tseng et al. 1994; Moestrup 1992; Suda 2003). However, *N. viridis* is different from these species with respect to pyrenoid and eyespot ultrastructure, flagellar length, and scale composition and architecture (Table 2). The closest relative of *N. viridis* is *N. olivacea*, a freshwater species and the type of the genus. The features shared by only *N. viridis* and *N. olivacea* are 1) a disc-like structure beneath the pyrenoid, 2) bipolar spiny body scales composed of 1-5-8-5-1 spines, 3) rod-shaped scales with tiny projections and 4) small stellate scales forming the third flagellar scale layer. In addition, the bean-shaped cells, the no. 1

flagellum coiling around the cell body at rest, the T-hairs with proximal subunits and the pyrenoid traversed by thylakoid sheets are also common to these two species. Molecular phylogenetic analysis also indicates their close relationship; however, *N. viridis* and *N. olivacea* are different in the shape of their starch sheath, the morphology of their second layer body scales, the number of subunits in their T- and P_1-hairs, the presence of a contractile vacuole and their habitat (Table 2). In addition, *N. viridis* cells are smaller and rounder than *N. olivacea* cells (Moestrup and Ettl 1979). The composition of their photosynthetic pigments is also distinct. Yoshii et al. (2005) reported that *N. viridis* (as *Nephroselmis* sp.3) had siphonaxanthin and its derivative pigments, while *N. olivacea* had none of these carotenoids. However, although siphonaxanthin and its derivatives are present in *N. viridis*, this species exhibits a more greenish color than *N. olivacea* (especially in wild samples; see Moestrup and Ettl 1979). Based on these results, we designate this new alga *Nephroselmis viridis* sp. nov. Since *N. viridis* was isolated from Japan, Fiji and South Africa, this alga is probably distributed all over the world, especially in temperate and tropical regions.

Interestingly, the different strains of *N. viridis* (NIES-486, PS535, MBIC 10871) show variation in the number of putative introns in their 18S rDNA (Fig. 8a). Because

the sequences of 18S rDNA excluding putative introns (this study) and the internal transcribed spacer (unpublished) are nearly identical, these strains obviously belong to the same species, and changes in the distribution of introns would have occurred in a short period. The sequences of the putative introns in the same site are nearly identical between NIES-486 and PS535. Thus, the putative introns in the same site are apparently homologous. Deletion or acquisition of introns, in addition to the variation in scales (see above), may be useful for studying the relationships among intraspecific populations of *N. viridis*. Variable intron distribution within a species has been reported in other eukaryotes (e.g., Perotto et al. 2000; Côté et al. 2004).

Phylogeny of *Nephroselmis* species

Because the marine species of *Nephroselmis* are apparently paraphyletic in the molecular phylogenetic tree, their common ancestor would probably have inhabited a marine environment. Thus, the invasion to freshwater would have occurred only once in *Nephroselmis* as in other 'prasinophycean' genera such as *Pyramimonas* and *Tetraselmis*.

N. viridis provides some insights into the evolution of the genus *Nephroselmis* (Fig. 9). Characters shared by only *N. viridis* and *N. olivacea* are probably synapomorphies of the two species. An outermost stellate flagellar scale was also reported in *N. rotunda* (Manton et al. 1965); however, that type of scale is restricted to the proximal region of the flagella, has a slightly different shape and is rather similar to the unipolar spiny body scales. The scale in *N. rotunda* is probably not a stellate flagellar scale but a unipolar spiny body scale. In addition, the pyrenoid matrix traversed by thylakoid sheets is also a common character of *N. viridis* and *N. olivacea*, although the route of the thylakoids is different. Thylakoid sheets intruding into the pyrenoid are also found in *N. astigmatica* (Inouye and Pienaar 1984), but the molecular phylogenetic analysis suggests that this feature is not a homologous but rather a homoplasious character. An ultrastructural difference in the pattern of thylakoid invagination is consistent with this suggestion: in *N. astigmatica*, the thylakoids invade the pyrenoid matrix and terminate in the matrix, whereas they exhibit a U-shaped path in *N. viridis*.

In the 18S rDNA tree, *N. spinosa* is a sister to the clade of *N. viridis* and *N. olivacea*. Although the statistical support for this position of *N. spinosa* is low, some morphological characters support this relationship. The symmetrical cells with the no. 1

flagellum coiling around cell body at rest and the T-hairs with proximal subunits are unique to the clade. Other species of *Nephroselmi* for which molecular data are not available, including *N. rotunda*, *N. minuta* and *N. gaoae,* are probably members of this clade, because they share the rounded cell shape and the coiling no. 1 flagellum. The clade of *N. anterostigmatica* and *N. astigmatica* is a sister to the clade including *N. spinosa*, *N. viridis* and *N. olivacea* in the 18S rDNA tree. The species in these clades, that is, all species of *Nephroselmis* excluding *N. pyriformis*, have the large spiny scales as a synapomorphy. Typically, they have large unipolar and bipolar large spiny scales, but the bipolar scale is sometimes diminished or missing, as in old cultures of *N. viridis* (this study) and *N. olivacea* (Moestrup and Ettl 1979). In addition, our study revealed significant variability in the size of the unipolar spiny scales among strains of *N. viridis* (Table 1). Such variety is also present within single strains and even within single cells (Nakayama et al. 2007; this study). The putative unipolar spiny scale in PS535 is very small (*c*. 100 nm in diameter), and it is similar to the small stellate body scale found in *N. pyriformis*, *N. anterostigmatica* and *N. rotunda* (Manton et al. 1965; Moestrup 1983; Nakayama et al. 2007).

All species of *Nephroselmis* excluding *N. pyriformis* have small, essentially square

innermost body scales. However, the morphology of these scales varies in these species. They are square Hanakaku type in *N. viridis* and *N. anterostigmatica*, Maltese cross type in *N. spinosa* and *N. olivacea* (and possibly *N. rotunda*; see Fig. 16 in Manton et al. 1965) and windmill type in *N. astigmatica* (Moestrup and Ettl 1979; Inouye and Pienaar 1984; Suda 2003; Nakayama et al. 2007). This variability is not congruent with the phylogenetic relationship suggested by the molecular phylogenetic analysis. However, the basic architecture of these scales is the same, that is, the scale has a central boss surrounded by four thickened corners. Possibly, these scale types arise from variations in thickness. The Hanakaku type, which is most similar to the underlayer square body scale, would be the basic form. Thickening (especially at corners) of the Hanakaku type would lead to the windmill type, and removal of material between the corners would lead to the Maltese cross type. The fact that Maltese cross scales are arranged diagonally to the underlayer square scales (Moestrup and Ettl 1979) suggests that the bars of the Maltese cross scale correspond to the corners of the Hanakaku scale, which supports our hypothesis. These small scales on the underlayer square scale would be a synapomorphy of the species of *Nephroselmis* excluding *N. pyriformis*, and convergent evolution of this type of scale probably occurred. Small stellate scales form the second

scaly layer on *N. pyriformis* cells (Moestrup 1983). However, this type of scale is apparently not homologous to the Hanakaku scale, because it is found on the Hanakaku scale of *N. anterostigmatica* (Nakayama et al. 2007) and on the Maltase cross scale of *N. rotunda* (Fig. 16 in Manton et al. 1965).

This study characterizes a marine species that is a sister to the freshwater type species of *Nephroselmis*. The detailed study of *N. viridis* provides some insights into the phylogeny and evolution of the Nephroselmidophyceae. However, it should be noted that many undescribed species of the genus remain. Further study of these species will help to elucidate the early evolution of Chlorophyta.

Acknowledgments

The initial stage of this work was done at the National Institute for Environmental Studies (NIES), Tsukuba, Japan. II is most grateful to Prof. Makoto M. Watanabe for providing an opportunity to stay and work in his laboratory at NIES. RNP warmly acknowledges the help of the staff of the Electron Microscope Unit of the Witwatersrand. This study was financially supported in part by a Grant-in-Aid for Scientific Research, Japan and the National Research Foundation, South Africa.

References

Burke JM, Belfort M, Cech TR, Davies RW, Schweyen RJ, Shub DA, Szostak JW, Tabak HF (1987) Structural conventions for group I introns. Nucleic Acids Res 15:7217-7221

Butcher RW (1959) An introductory account of the smaller algae of British coastal waters. Part I. Introduction and Chlorophyceae. Fisheries Investigations 4: 1-74

Carter N (1937) New or interesting algae from brackish water. Arch Protistenk 90: 1-68

Cavalier-Smith T (1993) The origin, losses and gains of chloroplast. In: Lewin RE (ed) Origin of Plastid: Symbiogenesis, Prochlorophytes and the Origins of Chloroplast. Chapman and Hall, New York, pp. 291-348

Côté MJ, Prud'homme M, Meldrum AJ, Tardif M-C (2004) Variations in sequence and occurrence of SSU rDNA group I introns in *Monilinia fructicola* isolates. Mycologia 96: 240–248

Ettl H, Moestrup Ø (1980) Light and electron microscopical studies on *Hafniomonas* gen. nov. (Chlorophyceae, Volvocales), a genus resembling *Pyramimonas* (Prasinophyceae). Pl Syst Evol 135: 177-210.

Fawley MW, Yun Y, Qin M (2000) Phylogenetic analyses of 18S rDNA sequences

reveal a new coccoid lineage of the Prasinophyceae (Chlorophyta). J Phycol 36: 387-393

Guillou L, Eikrem W, Chrétiennot-Dinet M-J, Le Gall F, Massana R, Romari K, Pedrós-Alió C, Vaulot D (2004.) Diversity of picoplanktonic prasinophytes assessed by direct nuclear SSU rDNA sequencing of environmental samples and novel isolates retrieved from oceanic and coastal marine ecosystems. Protist 155:193-214

Haugen P, Simon DM, Bhattacharya D (2005) The natural history of group I introns. Trends Genet 21: 111-119

Hansen G, Moestrup Ø (1998) Fine-structural characterization of *Alexandrium catenella* (Dinophyceae) with special emphasis on the flagellar apparatus. Europ J Phycol 33:281–291

Hoffman LR (1967) Observations on the fine structure of *Oedogonium*. III. Microtubular element in the chloroplast of *Oe. cardiacum*. J Phycol 3: 212–221

Holmes JA, Dutcher SK (1989) Cellular asymmetry in *Chlamydomonas reinhardtii*. J Cell Sci 94:273–285

Honda D, Inouye I (1995) Ultrastructure and reconstruction of the flagellar apparatus

architecture in *Ankylochrysis lutea* (Chrysophyceae, Sarcinochrysidales). Phycologia 34: 215–27

Hori T, Inouye I, Horiguchi T, Boalch GT (1985) Observations on the motile stage of *Halosphaera minor* Ostenfeld (Prasinophyceae) with special reference to the cell structure. Bot Mar 28: 529–538

Hori T, Moestrup Ø, Hoffman LR (1995) Fine structural studies on an ultraplanktonic species of *Pyramimonas*, *P. virginica* (Prasinophyceae), with a discussion of subgenera within the genus *Pyramimonas*. Eur J Phycol 30: 219–234

Inouye I, Pienaar RN (1984) Light and electron microscope observations on *Nephroselmis astigmatica* sp. nov. (Prasinophyceae). Nord J Bot 4: 409-423

Inouye I, Hori T (1991) High-speed video analysis of the flagellar beat and swimming patterns of algae: possible evolutionary trends in green algae. Protoplasma 164: 54-69

Inouye I, Hori T, Chihara M (1990) Absolute configuration analysis of the flagellar apparatus of *Pterosperma cristatum* (Prasinophyceae) and consideration of its phylogenetic position. J Phycol 26: 329–344

Johansen S, Haugen P (2001) A new nomenclature of group I introns in ribosomal DNA.

RNA 7: 935–936

Kasai F, Kawachi M, Erata M, Mori F, Yumoto K, Sato M, Ishimoto M (2009) NIES-Collection. List of Strains, 8th Edition. Jpn J Phycol (Sôrui) 57 Suppl.: 1–350

Lechtreck KF, Melkonian M (1991) An update on fibrous flagellar roots in green algae. Protoplasma 164: 38-44

Manton I, Rayns DG, Ettl H, Parke M (1965) Further observations on green flagellates with scaly flagella: the genus *Heteromastix* Korschikov. J Mar Biol Ass UK 45: 241-255

Marin B, Melkonian M (1994) Flagellar hairs in prasinophytes (Chlorophyta): ultrastructure and distribution on the flagellar surface. J Phycol 30: 659-678

Marin B, Melkonian M (1999) Mesostigmatophyceae, a new class of streptophyte green algae revealed by SSU rRNA sequence comparisons. Protist 150: 399-417

Marin B, Melkonian M (2009) Molecular phylogeny and classification of the Mamiellophyceae class. nov. (Chlorophyta) based on sequence comparisons of the nuclear- and plastid-encoded rRNA operons. Protist doi:10.1016/j.protis.2009.10.002

Massjuk NP (2006) Chlorodendrophyceae class. nov. (Chlorophyta, Viridiplantae) in the ukrainian flora: I. The volume, phylogenetic relations and taxonomical status. Ukr Bot J 63: 601-614

Melkonian M (1980) Ultrastructural aspects of basal body associated fibrous structures in green algae: a critical review. BioSystems 12: 85–104

Melkonian M (1984) Flagellar apparatus ultrastructure in relation to green algal classification. In: Irvine DE, John DM (eds) Systematics of the green algae. Academic Press, New York, pp 73–120

Melkonian M (1989) Flagellar apparatus ultrastructure in *Mesostigma viride* (Prasinophyceae). Plant Syst Evol 164: 93–122

Melkonian M (1990) Phylum Chlorophyta: Class Prasinophyceae. In: Margulis L, Corliss JO, Melkonian M, Chapman DJ (eds) Handbook of protoctista. Jones & Bartlett Publishers, London and Orland, pp. 600-607

Melkonian M, Reize IB, Preisig HR (1987) Maturation of a flagellum/basal body requires more than one cell cycle in algal flagellates: studies on *Nephroselmis olivacea* (Prasinophyceae). In: Wiessner W, Robinson DG, Starr RC (eds) Algal development, molecular and cellular aspects. Springer, Berlin Heidelberg New

York Tokyo, pp 102–113

Moestrup Ø (1978) On the phylogenetic validity of the flagellar apparatus in green algae and other chlorophyll *a* and *b* containing plants. BioSystems 10: 117–144

Moestrup Ø (1983) Further studies on *Nephroselmis* and its allies (Prasinophyceae). I. The question of the genus *Bipedinomonas*. Nord J Bot 3: 609–627

Moestrup Ø (1984) Further studies on *Nephroselmis* and its allies (Prasinophyceae). II. *Mamiella* gen. nov., Mamiellaceae fam. nov., Mamiellales ord. nov. Nord J Bot 4: 109–121

Moestrup Ø (1992) Prasinophyceae og andre grønne flagellater. In: Thomsen HA (ed) Havforskning fra Miljøstyrelsen. Nr. 11. Plankton I de indre danske farvande. Miljøstyrelsen, København, pp. 267–310

Moestrup Ø (2000) The flagellar cytoskeleton. Introduction of a general terminology for microtubular flagellar roots in protists. In: Leadbeater BSC, Green JC (eds) The Flagellates. Unity, Diversity and Evolution. Taylor & Francis Limited, London and New York, pp. 69–94

Moestrup Ø, Ettl H (1979) A light and electron microscopical study of *Nephroselmis olivacea* (Prasinophyceae). Opera Botanica 49: 1-40

Moestrup Ø, Hori T (1989) Ultrastructure of the flagellar apparatus of in *Pyramimonas octopus* (Prasinophyceae). II. Flagellar roots, connecting fibers and numbering of individual flagella in green algae. Protoplasma 148: 41-56

Moestrup Ø, Throndsen J (1988) Light and electron microscopical studies on *Pseudoscourfieldia marina*, a primitive scaly green flagellate (Prasinophyceae) with posterior flagella. Can J Bot 66: 1415-1434

Nakada T, Suda S, Nozaki H (2007) A taxonomic study of *Hafniomonas* (Chlorophyceae) based on a comparative examination of cultured material. J. Phycol. 43: 397–411

Nakayama T, Inouye I (2000) Ultrastructure of the biflagellate gametes of *Collinsiella cava* (Ulvophyceae, Chlorophyta). Phycol Res 48: 63–73

Nakayama T, Kawachi M, Inouye I (2000) Taxonomy and the phylogenetic position of a new prasinophycean alga, *Crustomastix didyma* gen. and sp. nov. (Chlorophyta). Phycologia 39: 337-348

Nakayama T, Marin B, Krantz HD, Surek B, Huss VAR, Inouye I, Melkonian M (1998) The basal position of scaly green flagellates among the green algae (Chlorophyta) is revealed by analyses of nuclear-encoded SSU rRNA sequences. Protist 149:

367-380

Nakayama T, Suda S, Kawachi M, Inouye I. (2007.) Phylogeny and ultrastructure of *Nephroselmis* and *Pseudoscourfieldia* (Chlorophyta), including the description of *Nephroselmis anterostigmatica* sp. nov. and a proposal for the Nephroselmidales ord. nov. Phycologia 46: 680–697.

Perotto S, Nepote-Fus P, Saletta L, Bandi C, Young JPW (2000) A diverse population of introns in the nuclear ribosomal genes of ericoid mycorrhizal fungi includes endonuclease-coding genes. Mol Biol Evol 17: 44–59

Pickett-Heaps JD (1968) Ultrastructure and differentiation in Chara (fibrosa). IV. Spermatogenesis. Australian Journal of Biological Sciences 21: 655–690

Pickett-Heaps JD, Fowke LR (1970) Mitosis, cytokinesis, and cell elongation in the desmid *Closterium littorale*. J Phycol 6: 189–215

Reynolds EC (1963) The use of lead citrate at high pH as an electron opaque stain in electron microscopy. J Cell Biol 17: 208-212

Skuja H (1948) Taxonomie des Phytoplanktons einiger Seen in Uppland, Schweden. Symb Bot Ups 9: 1-399

Sluiman HJ (1983) The flagellar apparatus of the zoospore of the filamentous green alga

Coleochaete pulvinata: Absolute configuration and phylogenetic significance. Protoplasma 115: 160-175

Spurr AR (1969) A low viscosity epoxy resin embedding medium for electron microscopy. J Ultrastructure Res 26: 31-42

Stamatakis A (2006) RAxML-VI-HPC: Maximum likelihood-based phylogenetic analyses with thousands of taxa and mixed models. Bioinformatics 22:2688–2690

Steinkötter J, Bhattacharya D, Semmelroth I, Bibeau C, Melkonian M (1994) Prasinophytes form independent lineages within the Chlorophyta: evidence from ribosomal RNA sequence comparisons. J Phycol 30: 340-345

Suda S (2003) Light microscopy and electron microscopy of *Nephroselmis spinosa* sp. nov. (Prasinophyceae, Chlorophyta). J Phycol 39: 590-599

Suda S, Watanabe MM, Inouye I (1989) Evidence for sexual reproduction in the primitive green alga *Nephoroselmis olivacea* (Prasinophyceae). J Phycol 25: 596-600

Suda S, Watanabe MM, Inouye I (2004) Electron microscopy of sexual reproduction in *Nephroselmis olivacea* (Prasinophyceae, Chlorophyta). Phycol Res 52: 273-283

Sym SD, Pienaar RN (1991) Light and electron microscopy of a punctate species of

Pyramimonas, *P. mucifera* sp. nov. (Prasinophyceae). J Phycol 27: 277–290

Sym SD, Pienaar RN (1993) The class Prasinophyceae. In: Round FE, Chapman DJ (eds) Progress in phycological research, vol. 9. Biopress Ltd., Bristol, pp. 281-376

Sym SD, Pienaar RN (1997) Further observations on the type subgenus of *Pyramimonas* (Prasinophyceae), with particular reference to a new species, *P. chlorina*, and the flagellar apparatus of *P. propulsa*. Can J Bot 75: 2196–2215

Tseng CK, Chen J, Zhang Z, Zhang H (1994) Light and electron microscope observations on *Nephroselmis gaoae* sp. nov. (Prasinophyceae). Chin J Oceanol Limnol 12: 201-207

Turmel M, Gagnon M-C, O'Kelly CJ, Otis C, Lemieux C (2009) The chloroplast genomes of the green algae *Pyramimonas*, *Monomastix*, and *Pycnococcus* shed new light on the evolutionary history of prasinophytes and the origin of the secondary chloroplasts of euglenids. Mol Biol Evol 26: 631–648

Viprey M, Guillou L, Ferréol M, Vaulot D (2008) Wide genetic diversity of picophytoplnaktonic green algae (Chloroplastida) in the Mediterranean Sea uncovered by a phylum-biased PCR approach. Environ Microbiol 10: 1804–1822

Yamaguchi H, Nakayama T, Murakami A, Inouye I (2010) Phylogeny and taxonomy of the Raphidophyceae (Heterokontophyta) and *Chlorinimonas sublosa* gen. et sp. nov., a new marine sand-dwelling raphidophyte. J Plant Res (In press)

Yoshii Y, Takaichi S, Maoka T, Suda S, Sekiguchi H, Nakayama T, Inouye I (2005) Variation of siphonaxanthin series among the genus *Nephroselmis* (Prasinophyceae, Chlorophyta), including a novel primary methoxy carotenoid. J Phycol 41: 827-834

Young AV, Pienaar RN (1989) The ultrastructure of a new species of *Nephroselmis* (Prasinophyceae). Proc Electron Microscopie Society of South Africa 19: 113–114

Figure legends

Fig. 1. Light micrographs (DIC) and schematic drawings of *Nephroselmis viridis* (NIES-486). **a** Right view of a cell at rest showing the eyespot (*small arrow*) and the no. 1 flagellum (*large arrowheads*) coiling around the cell body. The *large arrow* indicates a pyrenoid. **b** Right view of a cell showing a wide sinus of the chloroplast and no. 1 (*large arrowheads*) and no. 2 (*small arrowhead*) flagella. **c** Anterior (or posterior) view of a cell showing a basal pyrenoid (*large arrow*). **d–g** Schematic drawings. Right view of a swimming cell (**d**) and right (**e**), ventral (**f**) and anterior (**g**) view of a resting cell.

Fig. 2. Electron micrographs of *N. viridis* (NIES-486), SEM (**d**) and TEM (the others, thin sections). **a** Right view of a cell showing a cup-shaped chloroplast with a dorsal pyrenoid and an anterior eyespot. Note the pyrenoid surrounded by a cup-shaped starch sheath and a dorsal bilayered disc-like structure. **b** Ventral view of a cell showing the right nucleus and two bundles of globular subunits (*arrows*). **c** Anterior view of a cell showing a shallow ventral groove. Note the right nucleus and left Golgi body. **d** Scanning electron micrograph of a cell viewed from the right-ventral side. Note the two

flagella emerging from the shallow ventral groove surrounded by four low projections (*asterisks*). **e** A small bulge of the chloroplast including tubular structures (*arrows*). **f** A pyrenoid with starch sheath and a bilayered disc-like structure. Note the isolated thylakoids in the pyrenoid matrix showing U-shaped tracks (*arrows*). *B1* no. 1 basal body, *B2* no. 2 basal body, *C* chloroplast, *D* disc-like structure, *E* eyespot, *F1* no. 1 flagellum, *F2* no. 2 flagellum, *M* mitochondrion, *m* microbody, N nucleus, *P* Pyrenoid, *S* starch sheath.

Fig. 3. Transmission electron micrographs of *N. viridis* (NIES-486), thin sections. **a** Ventral view of a cell showing the right nucleus and left Golgi body with vesicles including scales (*arrowhead*). Note a cisterna from the nuclear envelope situated at the forming face of the Golgi body. **b, c** Longitudinal (**b**) and transverse (**c**) sections of the bundle of rows composed of globular subunits.

Fig. 4. Transmission electron micrographs of *N. viridis* scales, whole mounts (**d, e**) and thin sections (others). **a–c** Cross (**a, b**) and grazing (**c**) cell surface sections showing scaly layers (NIES-486). **d** Whole mount of spiny scales with 11 and 20 spines

(*asterisks*) (NIES-486). **e** Grazing cell surface section showing a small unipolar spiny scale (PS535). **f** Whole mount of thin unipolar spiny scales (MBIC 10871). **g, h** Cross (**g**, SA) and grazing (**h**, NIES-486) sections of flagella showing scaly layers. *Arrows* indicate T-hairs. *F* flagellum, *S1* innermost square scale, *S2* Hanakaku scale, *S3* unipolar spiny scale, *S4* bipolar spiny scale, *s1* pentagonal scale, *s2* rod-shaped scale, *s3* small stellate scale.

Fig. 5. Schematic drawings of *N. viridis* scales (NIES-486). **a–d** Body scales: innermost square scale (**a**), Hanakaku scale (**b**), unipolar spiny scale with 11 spines (**c**) and bipolar spiny scale with 20 spines (**d**). **e–g** Flagellar scales: pentagonal scale (**e**), rod-shaped scale (**f**) and small stellate scale (**g**).

Fig. 6. Transmission electron micrographs of *N. viridis* scales, whole mounts. **a** A cell showing a long no. 1 flagellum (*F1*) and a short no. 2 flagellum (*F2*). Note the T-hairs attached to both flagella and the P_1-hairs (*arrows*) adhering to only the no. 2 flagellum. **b–f** T-hairs of NIES-486 (**b**), PS535 (**c**), MBIC 10871 (**d**), SA (**e**) and Saeki-L (**f**). Bars indicate junctions between proximal filaments (only **b**), shafts, proximal subunits, distal

subunits and terminal filaments (only **b**). **g, h** P_1-hairs of NIES-486 (**g**) and Saeki-L (**h**). Bars indicate junctions between proximal wedges (only **g**), shafts, central subunits and distal subunits.

Fig. 7. Schematic drawings of *N. viridis* hair scales (NIES-486). **a** T-hair composed of a proximal filament (*I*), a shaft (*II*), proximal subunits (*III*), distal subunits (*IV*) and a distal filament (*V*). **b** P_1-hair composed of a proximal wedge (*I*), a shaft (*II*), central subunits (*III*) and distal subunits (*IV*).

Fig. 8. a Map of 18S rDNA and intron insertions in three strains of *N. viridis*. **b** Phylogenetic tree based on 18S rDNA sequences using the maximum likelihood method (-ln *L* = 5422.594372). The tree was inferred using the GTRMIX model by RAxML ver. 4.03 (Stamatakis 2006). The tree is rooted on the branch between *Nephroselmis* and the outgroups (*Pyramimonas*, *Pseudoscourfieldia*). The numbers above the internodes indicate the bootstrap values in the ML analysis (100 replications). Only bootstrap values ≥50% are given.

Fig. 9. Phylogenetic relationship and possible character changes of *Nephroselmis*. **Node 1** (genus *Nephroselmis*): Cell compressed in right–left axis; type I cell (see Table 2); scaly body covering composed of square and small stellate scales; no transitional plate on the stellate structure; pyrenoid matrix intruded by tubular thylakoids; cup-shaped starch sheath; type I carotenoids (*sensu* Yoshii et al. 2005). **Node 2**: Specialized T-hair on the tip of no. 1 flagellum (tip hair). **Node 3**: Hanakaku scales or their derivatives; unipolar large spiny scales (1-5-5 spines); bipolar large spiny scales (1-5-4-5-1 spines?). **Node 4**: Large amounts of α-carotene; γ-carotene. **Node 5**: Anterior eyespot. **Node 6**: type II cell (see Table 2); loss of eyespot; pyrenoid matrix traversed by thylakoid sheets; loss of small stellate body scales; large spiny scales with 1-4-4-4-8 and 1-4-4-4-4-4-1 spines; pit scales; pit hairs. **Node 7**: Type III cell (see Table 2); no. 1 flagellum coiling around cell at rest; T-hairs with proximal subunits; distinct transitional plate on stellate structure; degeneration of normal basal plate; loss of 6'-siphonaxanthin ester; relatively large amount of β-carotene. **Node 8**: Sword-like scales; R-hairs; tripartite starch sheath. **Node 9**: Pyrenoid matrix traversed by thylakoid sheets; disc-like structure beneath the pyrenoid; degeneration of the normal transitional plate; bipolar spiny scales with 1-5-8-5-1 spines; spiny stellate flagellar scales; large amount of lutein. **Node 10**:

Siphonaxanthin C14:1 ester. **Node 11**: Bilenticular starch sheath; loss of siphonaxanthin and its derivatives; contractile vacuole; freshwater habitat.

Table 1. Morphological characters of *N. viridis* strains. BSS = bipolar spiny scale, USS = unipolar spiny scale, NS = not studied.

Strain	NIES-486	PS535	MBIC 10871	SA	Saeki-L
Locality	Japan	Japan	Fiji	South Africa	Japan
1st layer body scales	Square	Square	Square	Square	Square
2nd layer body scales	Hanakaku	Hanakaku	Hanakaku	Hanakaku	Hanakaku
USS spines	1-5-5	1-5-5	1-5-5	1-5-5	1-5-5
Size of USSs (nm)	180	100	180	180	180
Spine thickness of USSs	Thick	Thin	Thin/Thick	Thick	Thick
BSS spines	1-5-8-5-1*	1-5-8-5-1	Absent	1-5-8-5-1	1-5-8-5-1
Size of BSSs (nm)	360*	360	–	360	360
Distribution of BSSs	All*	All	–	All	Groove
1st layer flagellar scales	Pentagonal	Pentagonal	Pentagonal	Pentagonal	Pentagonal
2nd layer flagellar scales	Rod-shaped	Rod-shaped	Rod-shaped	Rod-shaped	Rod-shaped
3rd layer flagellar scales	Stellate	Stellate	Stellate	Stellate	Stellate
No. proximal subunits in T-hairs	11	11	10	12	10
No. distal subunits in T-hairs	20	22	18	20	20
No. central subunits in P_l-hairs	17	NS	NS	NS	19
No. distal subunits in P_l-hairs	56	NS	NS	NS	65
Introns in 18S rDNA	S324, S989	S324, S959, S989	Absent	NS	NS

*Absent in the strain after 1990'.

Table 2. Comparison of selected characters among *Nephroselmis* species.

	N. pyriformis[*1]	*N. anterostigmatica*[*2]	*N. astigmatica*[*3]	*N. rotunda*[*4]	*N. minuta*[*5]	*N. gaoae*[*6]	*N. spinosa*[*7]	*N. viridis*[*8]	*N. olivacea*[*9]
Cell shape[*10]	Type I	Type I	Type II	Type III	Type III	Type III	Type III	Type III	Type III
No. 1 flagellum at rest	Extending	Extending	Extending	Coiling[*13]	Coiling	Coiling	Coiling	Coiling	Coiling
2nd square body scales	Absent	Hanakaku	Windmill	Maltese cross	Absent (?)	Absent (?)	Maltese Cross	Hanakaku	Maltese Cross
Small stellate body scales	Present	Present	Absent	Present (?)	Present (?)	Present	Absent	Absent	Absent
Unipolar spiny scales	Absent	1-5-5	1-4-4-4-8	1-5-5 (1-4-4?)	1-5-5	1-4-4(-4) (?)	1-5-5	1-5-5	1-5-5
Bipolar spiny scales	Absent	1-5-4-5-1	1-4-4-4-4-4-1	Absent	Absent	Absent	Absent	1-5-8-5-1	1-5-8-5-1
Pit scales	Absent	Absent	Present	Absent	?	?	Absent	Absent	Absent
Distinct projections of rod-shaped scales	Absent	Absent	Absent		?	?	?	Present	Present
Stellate flagellar scales	Absent	Absent	Absent	Absent (?)[*12]	Present (?)	Absent (?)	Absent	Present	Present
No. subunits in T-hairs (proximal/distal)	0/12–16	0/27–31	0/4	0/32	?	?	14/29	10–12/18–23	11–29/10–28
No. subunits in Pl-hairs (central/distal)	18–24/44–56	5–24/55–99	21/47	17/49	?	?	14/53	17–19/56–65	19–26/53–75
Pit hair	Present	Absent	Present	?	?	?	Present (R-hair)	Absent	Absent
Tip hair	Present	Absent	Absent	?	?	?	Absent	Absent	Absent
Starch sheath	Cup	Cup	Cup	Cup	?	Continuous	Tripartite	Cup	Bilenticular
Thylakoids in pyrenoid	Tube	Tube	Sheet	Tube	?	Tube	Absent	Sheet	Sheet
γ-carotene[*11]	Absent	6	2	?	?	?	Absent	Absent	Absent
β-carotene[*11]	Absent	<1	Absent	?	?	?	3–8	15–21	12
α-carotene[*11]	3	27	20	?	?	?	<1	<1	Absent
Lutein[*11]	2	3	1	?	?	?	41–44	8–33	59
19-methoxy siphonaxanthin[*11]	Absent	Absent	Absent	?	?	?	Absent	5–13	Absent
Siphonaxanthin C12:1 ester[*11]	<1	4	2	?	?	?	2–3	2–9	Absent
Siphonaxanthin C14:1	31	24	23	?	?	?	Absent	<6	Absent

ester[*11]									
6'-OH siphonaxanthin C12:1 ester[*11]	2	7	1	?	?	?	Absent	Absent	Absent
6'-OH siphonaxanthin C14:1 ester[*11]	26	10	25	?	?	?	Absent	Absent	Absent
Eyespot	Anterior-ventral	Anterior	Absent	Anterior-ventral	Anterior-ventral	Anterior-ventral (rod-shaped subunits)	Anterior-ventral	Anterior-ventral	Anterior-ventral
Contractile vacuole	Absent	Absent	Absent	Absent	Absent	Absent	Absent	Absent	Present
Habitat	Marine	Marine	Marine	Marine	Marine	Marine	Marine	Marine	Freshwater

? Unknown character. [*1] Moestrup (1983), Marin and Melkonian (1994), Nakayama et al. (2007). [*2] Nakayama et al. (2007). [*3] Inouye and Pienaar (1984), Nakayama et al. (2007). [*4] Manton et al. (1965), Marin and Melkonian (1994). [*5] Moestrup (1992). [*6] Tseng et al. (1994) *7 Suda (2003) [*8] This study [*9] Moestrup and Ettl (1979), Marin and Melkonian (1994). [*10] Type 1 = Obovate cell asymmetrical in both anterior–posterior and right–left axes. Type II = Ovate cell asymmetrical in right–left axis. Type III = Bean-shaped cell symmetrical in both anterior–posterior and right–left axes. [*11] mol% of total carotenoids, Yoshii et al. (2005). [*12] This scale is restricted at the proximal part of the flagella. [*13] Butcher (1959) noted extending no. 1 flagellum at rest.

Fig. 1

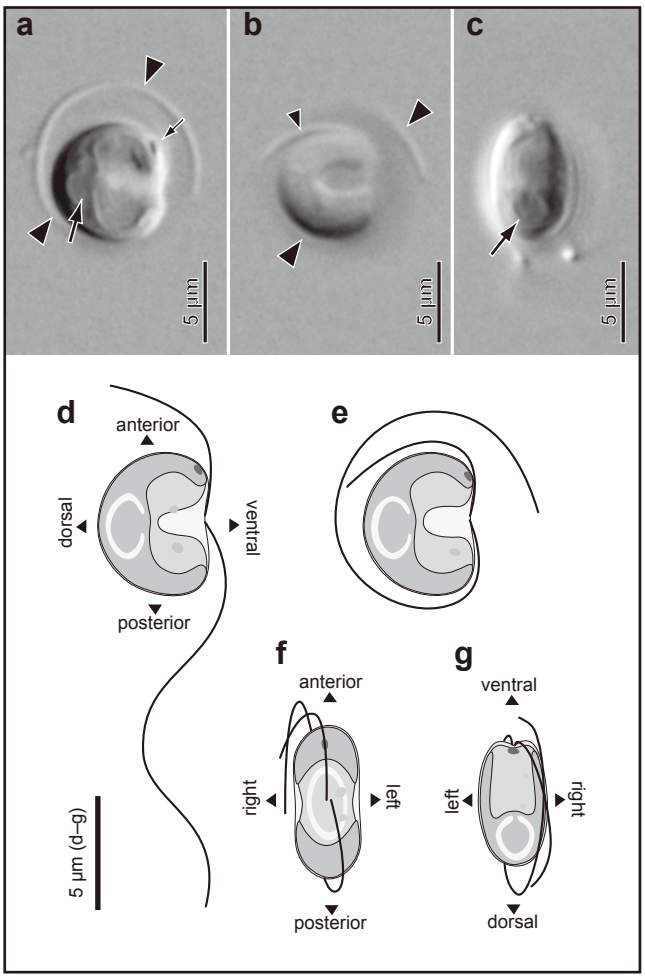
a
b
c
5 µm
5 µm
5 µm
d
anterior
dorsal
ventral
posterior
e
f
anterior
right
left
posterior
g
ventral
left
right
dorsal
5 µm (d–g)

Fig. 2

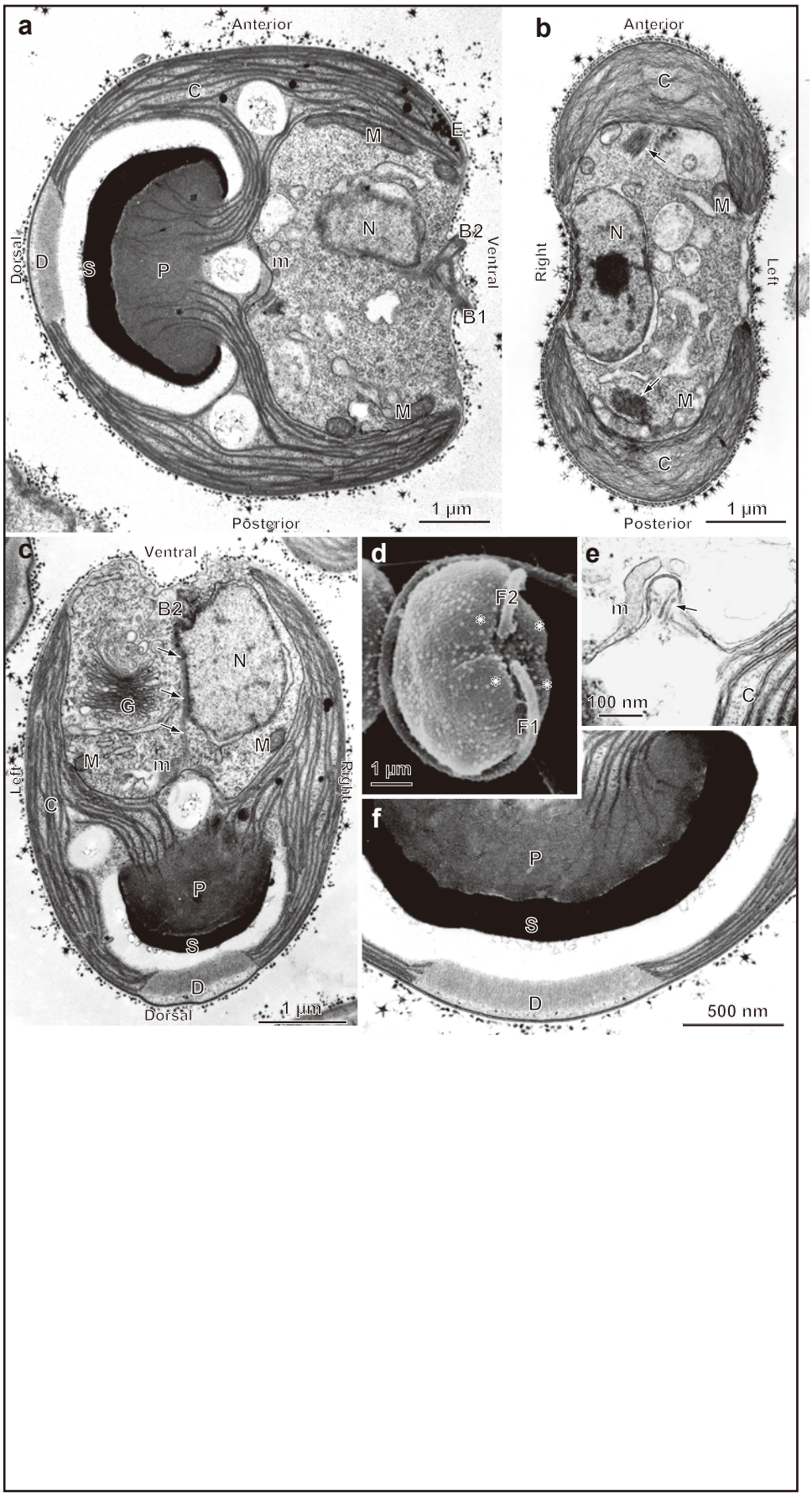
a
Anterior
C
M
E
N
B2
Ventral
Dorsal
D
S
P
m
B1
M
Posterior
1 µm
b
Anterior
C
M
N
Right
Left
M
C
Posterior
1 µm
c
Ventral
B2
N
G
M
M
m
Left
Right
C
P
S
D
Dorsal
1 µm
d
F2
F1
1 µm
e
m
100 nm
C
f
P
S
D
500 nm

Fig. 3

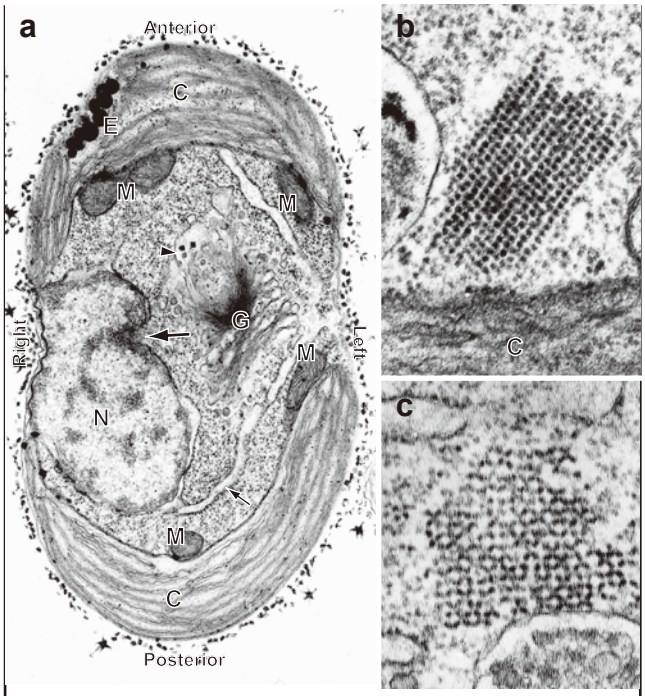

Fig. 4

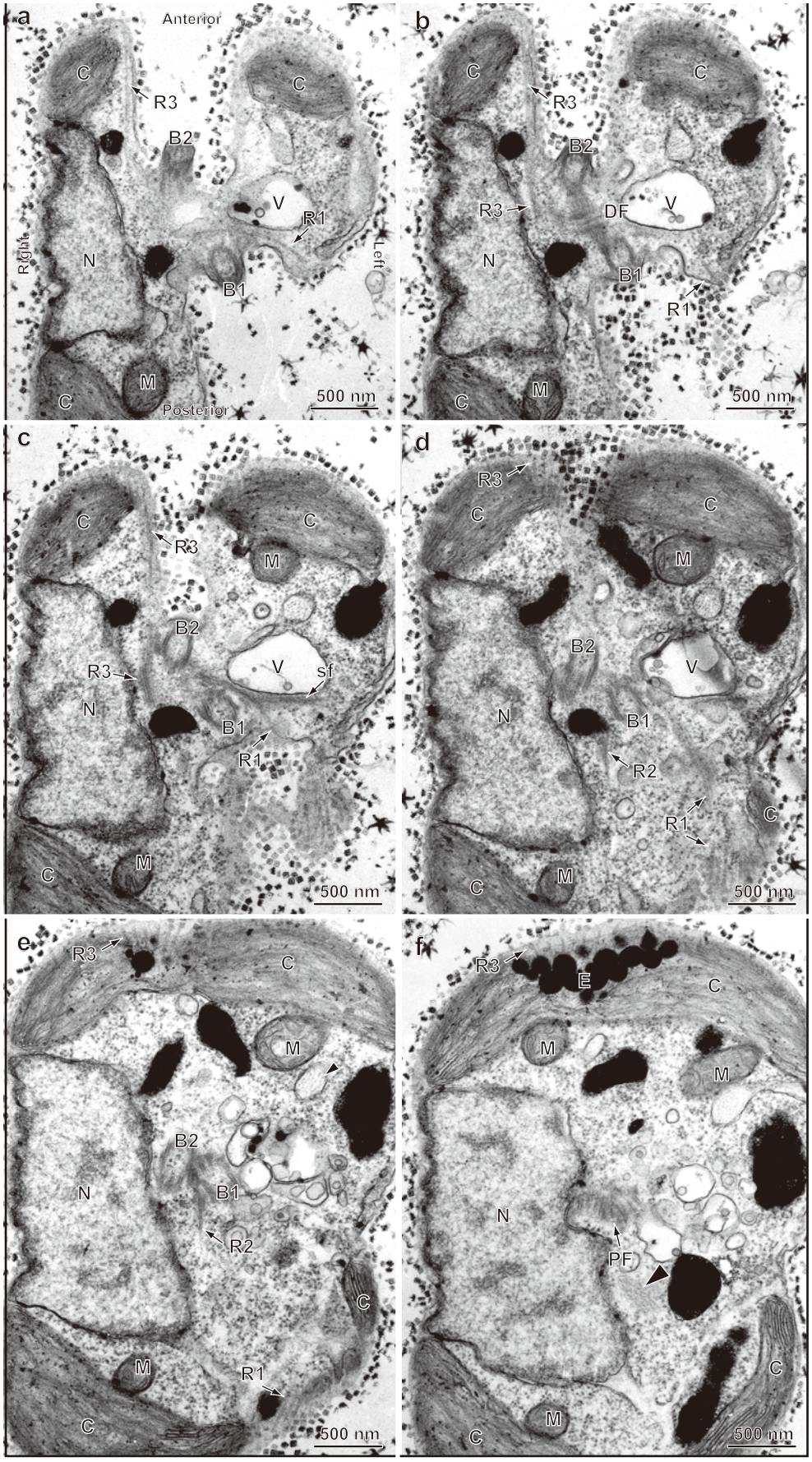
a
Anterior
C
R3
C
B2
V
R1
Right
Left
N
B1
M
C
Posterior
500 nm
b
C
R3
C
B2
R3
DF
V
N
B1
R1
C
M
500 nm
c
C
R3
C
M
B2
R3
V
sf
N
B1
R1
C
M
500 nm
d
R3
C
C
M
B2
V
N
B1
R2
R1
C
C
M
500 nm
e
R3
C
M
B2
N
B1
R2
C
M
R1
C
500 nm
f
R3
E
C
M
M
N
PF
C
C
M
500 nm

Fig. 5

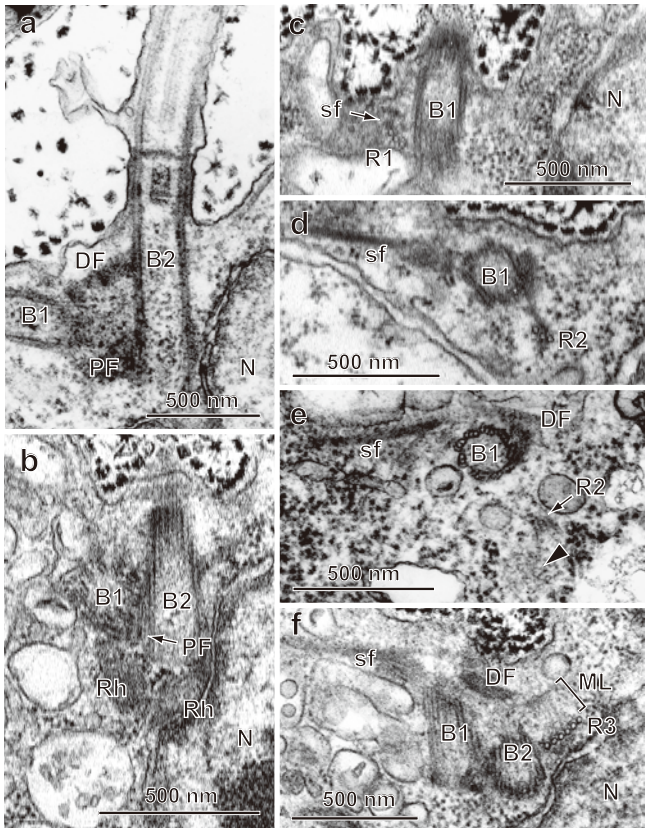
a
DF
B2
B1
PF
N
500 nm
b
B1
B2
PF
Rh
Rh
N
500 nm
c
sf
B1
N
R1
500 nm
d
sf
B1
R2
500 nm
e
DF
sf
B1
R2
500 nm
f
sf
DF
ML
R3
B1
B2
N
500 nm

Fig. 6

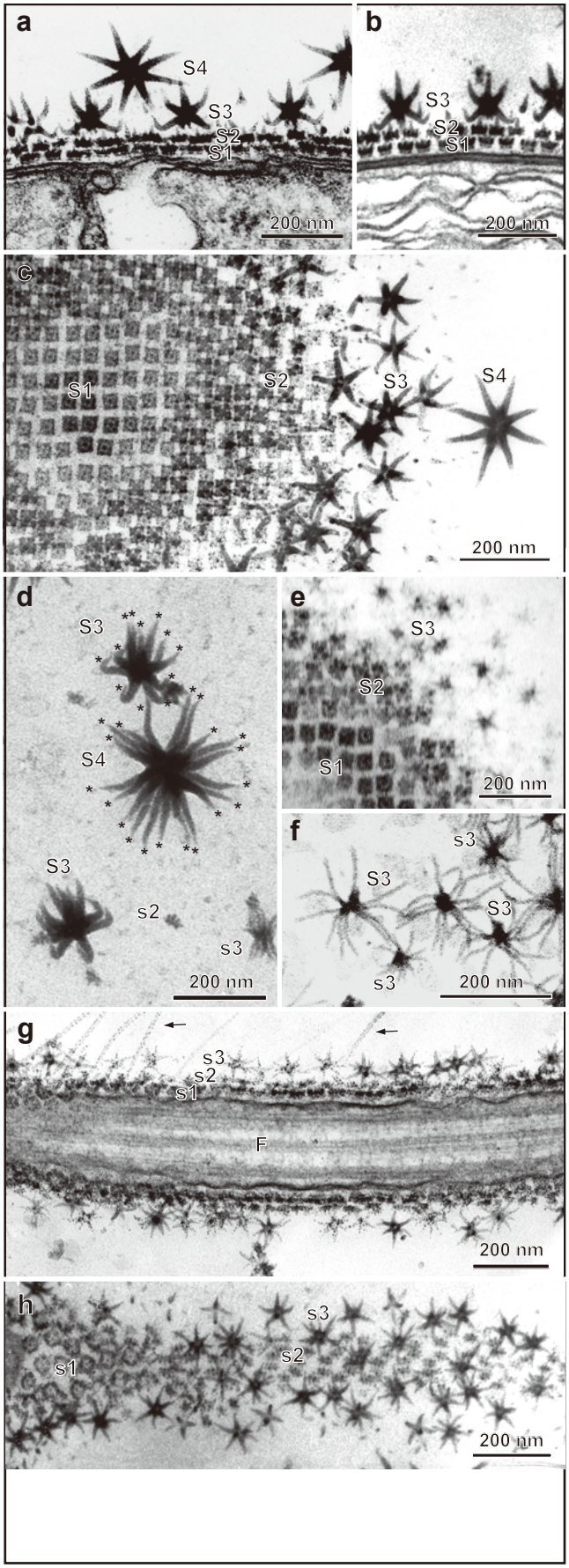
a
S4
S3
S2
S1
200 nm
b
S3
S2
S1
200 nm
c
S1
S2
S3
S4
200 nm
d
S3
S4
S3
s2
s3
200 nm
e
S3
S2
S1
200 nm
f
s3
S3
S3
s3
200 nm
g
s3
s2
s1
F
200 nm
h
s3
s2
s1
200 nm

Fig. 7

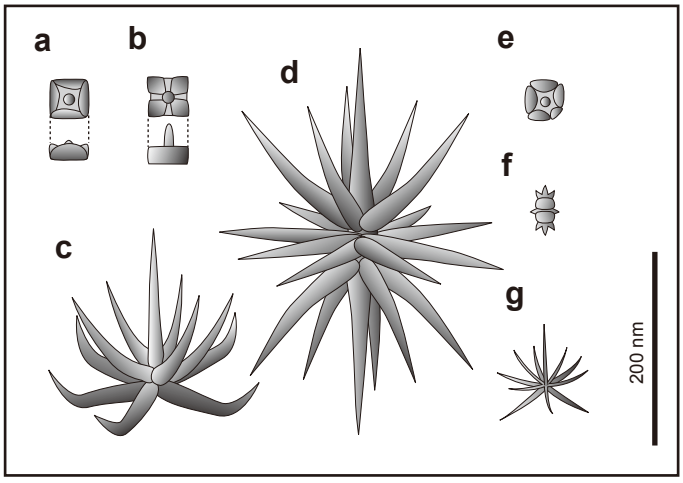

Fig. 8

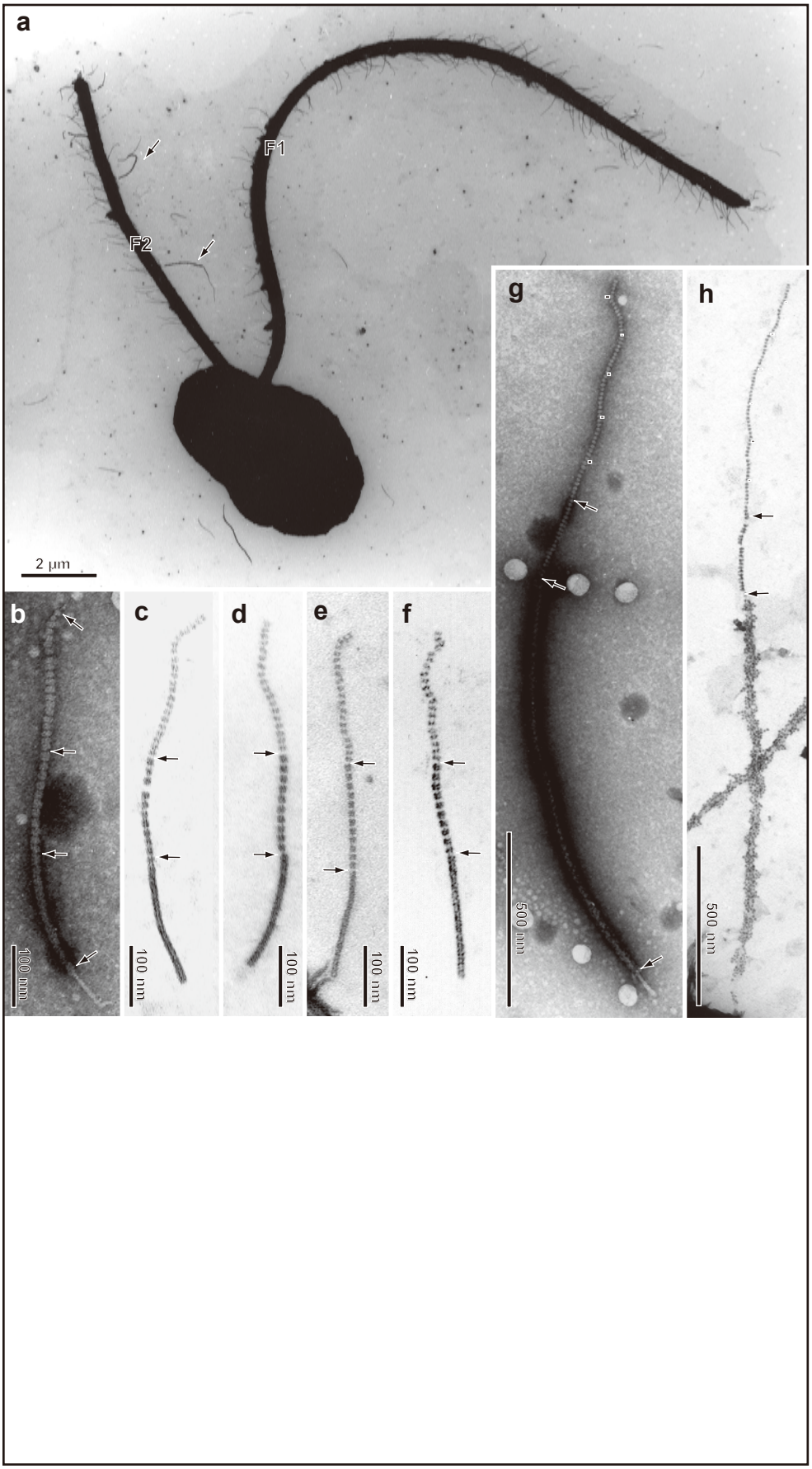
a
F1
F2
2 µm
b
100 nm
c
100 nm
d
100 nm
e
100 nm
f
100 nm
g
500 nm
h
500 nm

Fig. 9

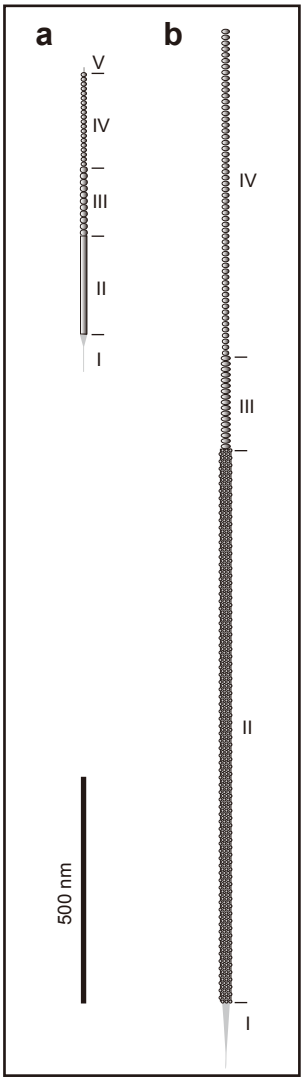

Fig. 10

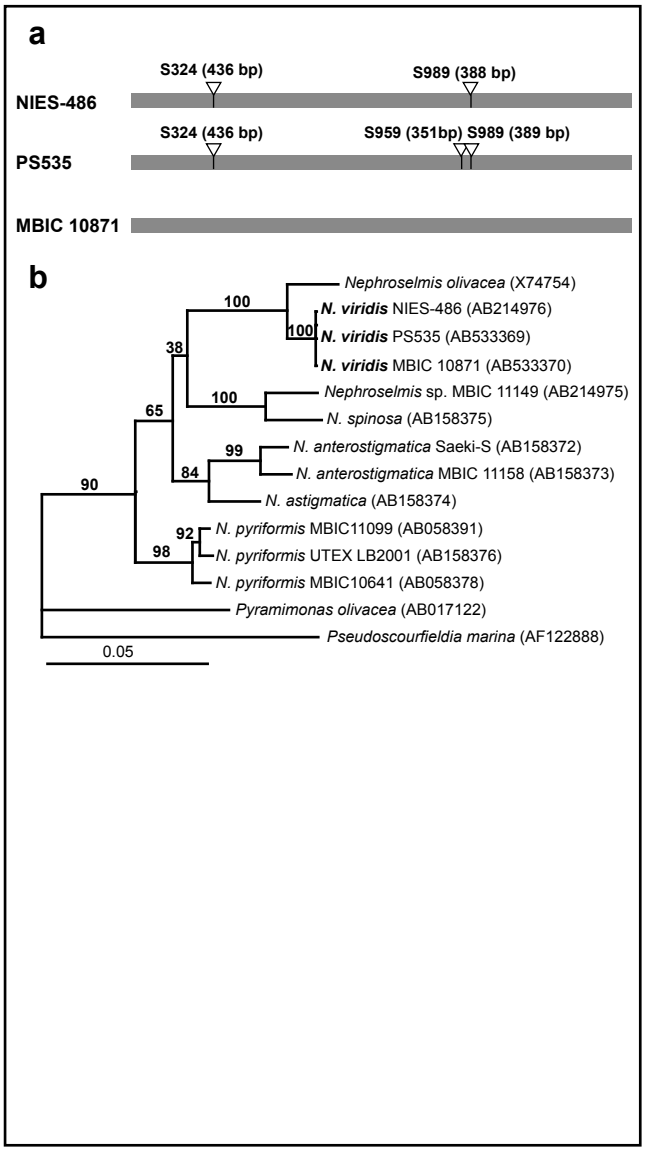
a
S324 (436 bp)
S989 (388 bp)
NIES-486
S324 (436 bp)
S959 (351bp) S989 (389 bp)
PS535
MBIC 10871
b
Nephroselmis olivacea (X74754)
N. viridis NIES-486 (AB214976)
N. viridis PS535 (AB533369)
N. viridis MBIC 10871 (AB533370)
Nephroselmis sp. MBIC 11149 (AB214975)
N. spinosa (AB158375)
N. anterostigmatica Saeki-S (AB158372)
N. anterostigmatica MBIC 11158 (AB158373)
N. astigmatica (AB158374)
N. pyriformis MBIC11099 (AB058391)
N. pyriformis UTEX LB2001 (AB158376)
N. pyriformis MBIC10641 (AB058378)
Pyramimonas olivacea (AB017122)
Pseudoscourfieldia marina (AF122888)
100
100
38
100
65
99
84
90
92
98
0.05

Fig.11

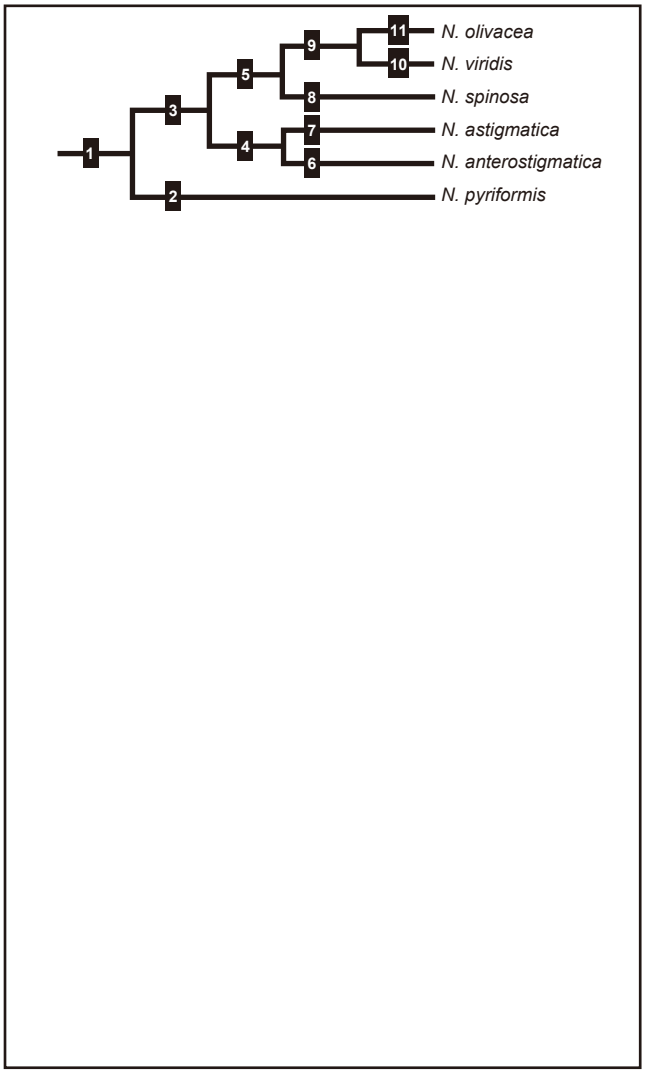
11
9
10
5
8
N. olivacea
N. viridis
N. spinosa
3
7
4
6
1
N. astigmatica
N. anterostigmatica
2
N. pyriformis